ACCURATE EXTRACTION OF DOPING PROFILES FROM ELECTROCHEMICAL CAPACITANCE VOLTAGE MEASUREMENTS

Robert Bock,[1] Pietro P. Altermatt[1,2] and Jan Schmidt[1]
[1]Institut für Solarenergieforschung Hameln (ISFH), Am Ohrberg 1, 31860 Emmerthal, Germany
[2]Dep. Solar Energy, Inst. Solid-State Physics, Leibniz University of Hannover, Appelstr. 2, 30167 Hannover, Germany

ABSTRACT:
It is known that the accuracy of Electrochemical Capacitance Voltage measurements crucially depends on many parameters such as measurement voltage, electrolyte concentration, the dissipation factor or the Debye length of the measured material. Using fully automated measurement equipment, we demonstrate that the accuracy is mainly determined by the precise knowledge of the Si-electrolyte contact area. The sealing rings used in commercially available ECV measurement equipment are not well defined and the contact area may increase during the measurement. We obtain a reproducible and excellent agreement between ECV, four-point probe, and SIMS measurements if we recalculate the doping profiles considering the exact Si-electrolyte contact area obtained from optical microscopy images. In addition, the corrected ECV data can be precisely reproduced with the process simulation software Ssuprem3.

1 INTRODUCTION

“Doping profile engineering” is a key word if an optimization of semiconductor devices is aimed. The common doping profile measurement methods are spreading resistance (SR), secondary ion mass spectroscopy (SIMS) and electrochemical capacitance-voltage (ECV). The SR method is simple and cheep but needs mechanical pretreatment of the sample and has restrictions in depth resolution [7-8]. The SIMS method is in comparison to the other methods expensive and provides only the chemical doping concentration, which is e.g. in the case of a phosphorus diffusion not very helpful for the use in simulations of electrical properties of semiconductor devices. In contrast, the ECV method provides only the electrically active dopants and has a depth resolution in the sub-nm range, which makes it a very powerful measurement tool for the use in device simulations and for device optimization in the PV industry [1]. However, today the ECV method, which is well known in the field of microelectronics, is still quite uncommon in photovoltaics, due to its limited accuracy. In this contribution, it is demonstrated that highly accurate results can be obtained from ECV measurements by applying relatively simple correction procedures.

2 EXPERIMENTAL

For the investigation of hole concentration profiles we use boron-diffused (100) oriented *n*-type FZ-Si wafers. The resulting p^+ diffusions have sheet resistances of 54 Ω/□ and 91 Ω/□. For the investigation of electron concentration profiles we use $POCl_3$ diffused *p*-type (100)-oriented textured and flat FZ-Si wafers with resulting sheet resistances of 38 Ω/□ and 95 Ω/□. The sheet resistances were measured using a four-point probe. The electrically active doping profiles from the boron- and phosphorus-doped samples are subsequently measured by the ECV technique using a WEP CVP21 profiler with a 0.1M solution of NH_4F. Good ohmic contact to the silicon was achieved using an Indium-Gallium alloy. For comparison, the dopant distributions of the boron-diffused samples are measured by means of Time-of-Flight Secondary Ion Mass Spectroscopy (TOF SIMS) using an IONOF TOFSIMS IV instrument in the depth profiling mode with Bi^+ analysis ions at 25 keV. Finally, we recalculate the measured doping profiles with exact area parameters obtained from optical microscopy images taken on the ECV-measured samples.

3 RESULTS

In commercially available automated measurement equipment, the ECV doping concentration is usually calculated from the electrochemical measurement assuming a fixed etch area, which is defined by the sealing ring geometry of the measurement equipment. In previous publications, it has been discussed that the etch crater wall is one major source of error in ECV measurements, whereas the Si-electrolyte contact area has always been assumed to be fixed since it is defined by the sealing ring geometry [6].

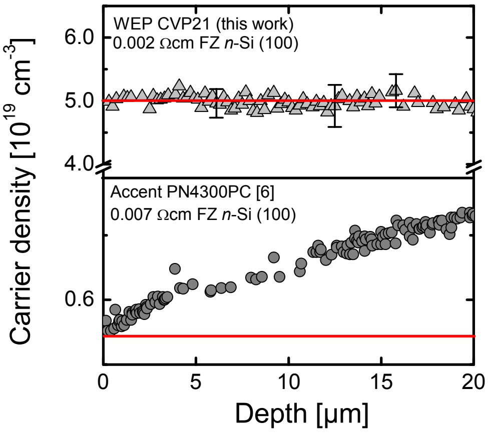

Figure 1: Comparison of ECV measurements on low-resistivity Si wafers using different measurement systems.

Figure 1 shows a comparison of ECV doping depth profiles of homogeneously doped low-resistivity *n*-type FZ-Si wafers measured with different measurement systems. It can be seen that the WEP CVP21 profiler shows a constant carrier concentration to a depth of 20µm. In comparison, the Accent PN4300PC shows a significant deviation of about 20% at this depth. We attribute the possible cause for this strong deviation to be a leakage of the sealing ring. The area contribution of the etch crater walls at an etch depth of 10 µm using a sealing ring of 3.5 mm in diameter is in the range of 1% and thus it is negligible especially for phosphorus and boron doping profile measurements. From optical microscopy analysis of the etch crater geometry directly after the ECV measurement with our equipment we found the Si-electrolyte contact area to be always larger by a factor of 1.16 – 1.18 than it is assumed for the calculation of the carrier concentration. This factor may be different with other commercially available ECV measurement equipment but is very like to be present. As a result of this Si-electrolyte contact area underestimation by the measurement system the carrier concentration is always overestimated in accordance with the Schottky-Mott equation.

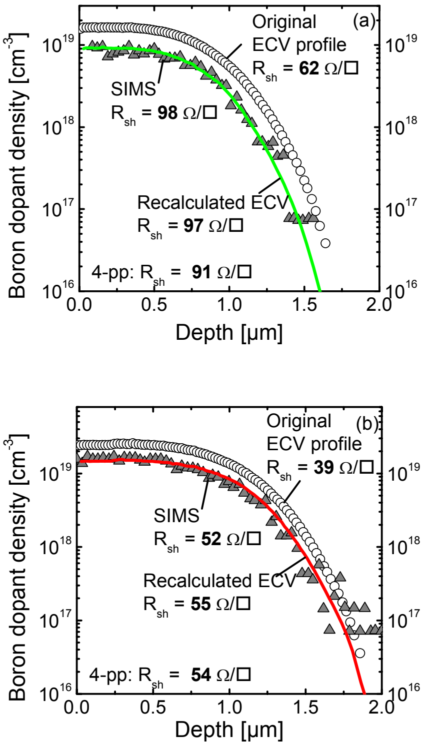

Figure 2: Boron-diffused samples with a sheet resistance of (a) 91 Ω/□ and (b) 54 Ω/□ measured by the four-point probe method.

Boron Diffusion

Figure 2 shows doping profiles measured on boron-diffused samples. Their sheet resistances are 91 Ω/□ [Figure 1 (a)] or 54 Ω/□ [Figure 1 (b)] as measured by the 4-pp technique. We use Masetti´s carrier mobility model [9] to calculate the sheet resistance of the original ECV doping profile: it is about 30% below that of the values measured by the 4-pp method. The sheet resistance obtained from the SIMS profile meets the 4-pp result within less than 10%. After the ECV doping profile has been recalculated with the 18% higher externally determined Si-electrolyte contact area, the resulting sheet resistance of 97 Ω/□ for the sample in Figure 2 (a) and 55 Ω/□ for the sample in Figure 2 (b) respectively, is in the range of the 4-pp measurement within less than 10%. Moreover, the corrected carrier distribution fits very well to the SIMS measurement as shown in Fig. 2 (a) and (b).

Phosphorus Diffusion

Figure 3 shows doping profile measurements of phosphorus-diffused samples with sheet resistances of 96 Ω/□ [Figure 2 (a)] and 40 Ω/□ [Figure 2 (b)] obtained from 4-pp measurements. The original ECV measurement again overestimates the 4-pp sheet resistance. The sheet resistance values from the ECV profile are again about 30% below that of the 4-pp measurement. This is not surprising since the same equipment has been used for the profile measurement, thus the Si-electrolyte contact area increased by the same amount (18%) resulting in an overestimated carrier concentration and, consequently, in a lower sheet resistance. Additionally, Ssuprem3 doping profile simulations are included in Fig. 3 where the diffusion parameters of the measured samples have been used for the calculation. The simulations show an excellent agreement with the corrected ECV doping profiles, proving that the parameterization method works also well for the carrier distribution, not only for the sheet resistance.

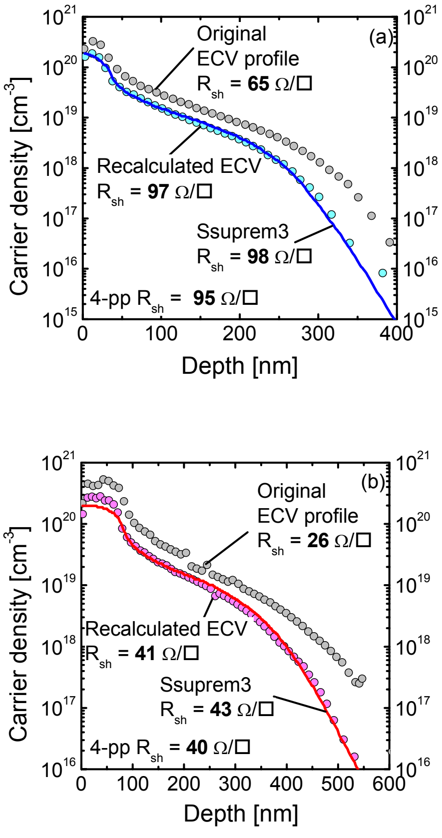

Figure 3: Phosphorus diffused samples with a sheet resisatance of (a) 95 Ω/□ and (b) 40 Ω/□ measured with a four-point probe.

However, the presented results have been obtained on flat samples. In order to apply this method to a non-flat sample, e.g., a random-pyramid-textured sample, the surface area enlargement due to the texture needs to be taken into account for the evaluation of the measured ECV profile. For a single-crystalline Si wafer textured with random pyramids, the average surface area enlargement is ~73%. Figure 4 shows ECV profiles of the same phosphorus diffusion on a textured sample and on a flat reference sample. It is quite clear that the original doping profile of the textured sample is completely erroneous due to the enlarged Si-electrolyte contact area and can not be used for device optimization nor for device simulation. In this case, the difference in sheet resistance between the ECV value of 5 Ω/□ and the 4-pp value of 24 Ω/□ is huge, whereas, as expected, the sheet resistance obtained from the 4-pp measurement for the textured sample and for the flat reference sample is nearly the same. After the profile of the reference sample has been recalculated using the enlarged contact area originating from the sealing ring a sheet resistance of 22 Ω/□ was determined, which is close to the 4-pp value. In order to extract the true doping profile of the textured sample, the enlargement factor is 1.18 × 1.73 = 2.04. As a result the sheet resistance determined from the recalculated ECV doping profile is about 25 Ω/□ and thus is in the range of the 4-pp value of 23 Ω/□ within 10 %.

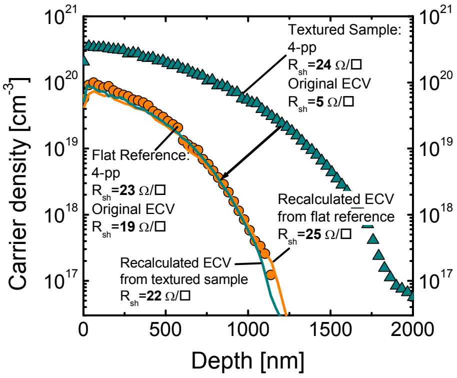

Figure 4: ECV doping profiles of phosphorus-diffused regions measured on flat reference samples and on random-pyramid-textured samples. The sheet resistances of both profiles match within 10% after recalculation using the corresponding Si-electrolyte contact area.

Application

The surface recombination parameter of minority carriers, S_{n0} or S_{p0}, is a measure for the quality of the surface passivation within the SRH recombination theory. At dopant-diffused surfaces this parameter is experimentally inaccessible and thus is numerically calculated from the measured saturation current-density J_{0e} of the diffused emitter. The procedure to extract S_{n0} is as follows. The J_{0e} values are obtained from QSSP measurements [10]. Then, J_{0e} is calculated as a function of the surface recombination velocity S_{n0}. We use the device simulator SENTAURUS [11] and the physical models described in Refs. 12 and 13. The surface recombination velocity parameter is the only free parameter in the model; other model parameters for Auger recombination, band gap narrowing, carrier mobilities etc. were independently determined and do not vary among experiments. Figure 5 shows that the simulated S_{n0} or S_{p0} values depend sensitively on the dopant profile: without the etch-area correction, too high dopant densities are measured, leading to an overestimation of Auger losses in the model.

The simulation where the original doping profile is used as input parameter shows a minimal J_{0e} of 60 fA/cm^2 at S_{n0} = 0 cm/s, which is higher than the measured J_{0e} of 55 fA/cm^2. Using the recalculated doping profile a realistic reproduction of the emitter saturation current density J_{0e} is achieved where the measured J_{0e} = 55 fA/cm^2 corresponds to S_{n0} = 2500 cm/s. An overestimated ECV doping profile generally leads to an overestimated J_{0e}.

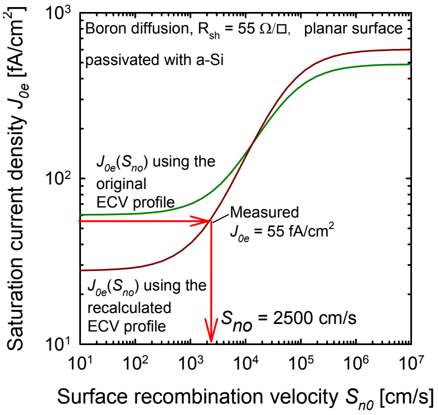

Figure 5: Simulated saturation current density J_{0e} as a function of the surface recombination velocity parameter S_{no} using the measured ECV profile before and after the correction procedure of a boron diffused region with a measured sheet resistance of R_{sh} = 55 Ω/□.

4 CONCLUSIONS

We have introduced a simple correction procedure for ECV doping profile measurements. An excellent agreement was found between the sheet resistance measured with the 4-point-probe method and that determined from the corrected ECV doping profiles (accuracy better ±10%). We have shown that the accuracy of ECV measurements is mainly determined by the precise measurement of the area of the electrolyte-Si contact. The corrected ECV doping profiles of the boron-diffused samples have been verified with secondary ion mass spectroscopy (SIMS) and were also found to be in excellent agreement.

In conclusion, we highly recommend an external etch area and crater depth determination and a recalculation of the measured ECV doping profile using this data in order to obtain accurate doping profiles suitable for advanced device simulations.

ACKNOWLEDGEMENT

Funding was provided by the State of Lower Saxony and the German Ministry for the Environment, Nature Conservation and Nuclear Safety (BMU) under Contract No. 0327666.

REFERENCES

[1] E. Peiner, *J.Electrochem.Soc.* **142** (1995) 576.

[2] T. Ambridge, C. R. Elliot, and M. M. Faktor, J. *Appl. Electrochem.,* 3, 1 (1973).

[3] P. Blood, *Semicond. Sci. TechnoI.,* 1, 7 (1986).

[4] K. Hansen, E. Peiner, A. Schlachetzki, W. MShling, and H. Menniger, *J. Cryst. Growth,* 125, 465 (1992).

[5] K. Hansen, E. Peiner, G.-P. Tang, A. Bartels, and A. Schlachetzki, *J. Appl. Phys.,* 76, 4705 (1994).

[6] F. Huster, and G. Schubert, *Proceedings of the 20th European Photovoltaic Solar Energy Conference, Barcelona, Spain* (WIP, Munich, 2005), p. 1462

[7] M. Pawlik, *J. Vac. Sci. Technol.,* B10, 388 (1992).

[8] S. R. Weinzierl, R. J. Hillard, J. M. Heddleson, P. Rai-Choudhury, R. G. Mazur, and C. M. Osburn, *ibid.,* B12, 322 (1994).

[9] Guido Masetti, Maurizio Severi, and Sandro Solmi, IEEE Transactions on Electron Devices, **30,** (1983) 764.

[10] D. E. Kane and R. M. Swanson, 18th IEEE PVSC, Las Vegas, 1985, p. 578.

[11] SENTAURUS, Synopsys Inc. Mountain View, CA, www.synopsys.com/products/tcad/tcad.html

[12] P. P. Altermatt et al., *J. Appl. Phys.,* 92, 3187 (2002).

[13] P. P. Altermatt et al, *Proceedings of the 21st European Photovoltaic Solar Energy Conference, Dresden, Germany* (WIP, Munich, 2006), p. 647.